Ring-Opening Reactions

Regioselectivity of Epoxide Ring-Openings via S$_N$2 Reactions Under Basic and Acidic Conditions

Thomas Hansen,[a,b][‡] Pascal Vermeeren,[a][‡] Anissa Haim,[a][+] Maarten J. H. van Dorp,[a][+] Jeroen D. C. Codée,[b] F. Matthias Bickelhaupt,*[a,c] and Trevor A. Hamlin*[a]
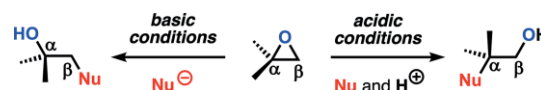
Abstract: We have quantum chemically analyzed the ring-opening reaction of the model non-symmetrical epoxide 2,2-dimethyloxirane under basic and acidic conditions using density functional theory at OLYP/TZ2P. For the first time, our combined activation strain and Kohn–Sham molecular orbital analysis approach have revealed the interplay of physical factors that control the regioselectivity of these chemical reactions. Ring-opening under basic conditions occurs in a regime of strong interaction between the nucleophile (OH$^-$) and the epoxide and the interaction is governed by the steric (Pauli) repulsion. The latter steers the attack preferentially towards the sterically less encumbered C$^\beta$. Under acidic conditions, the interaction between the nucleophile (H$_2$O) and the epoxide is weak and, now, the regioselectivity is governed by the activation strain. Protonation of the epoxide induces elongation of the weaker (CH$_3$)$_2$C$^\alpha$–O bond, and effectively predistorts the substrate for the attack at the sterically more hindered side, which goes with a less destabilizing overall strain energy. Our quantitative analysis significantly builds on the widely accepted rationales behind the regioselectivity of these ring-opening reactions and provide a concrete framework for understanding these indispensable textbook reactions.

Introduction

Epoxides constitute an important functional group in synthetic chemistry. Their easy availability and capability to react with a broad range of nucleophiles, including *C*-, *N*-, and *O*-nucleophiles, hydrides, and halides, renders epoxides valuable and versatile substrates in a myriad of organic transformations.[1] For this reason, these species have been frequently employed for the generation of synthetically valuable target molecules, including complex natural products, for medicinal and biochemical purposes.[2]

[a] T. Hansen, P. Vermeeren, A. Haim, M. J. H. van Dorp,
Prof. Dr. F. M. Bickelhaupt, Dr. T. A. Hamlin
Department of Theoretical Chemistry, Amsterdam Institute of Molecular
and Life Sciences (AIMMS), Amsterdam Center for Multiscale Modeling
(ACMM), Vrije Universiteit Amsterdam,
De Boelelaan 1083, 1081 HV Amsterdam, The Netherlands.
E-mail: t.a.hamlin@vu.nl
        f.m.bickelhaupt@vu.nl
https://trevorhamlin.weebly.com
http://www.few.vu.nl/~bickel/
[b] T. Hansen, Dr. J. D. C. Codée
Leiden Institute of Chemistry, Leiden University,
Einsteinweg 55, 2333 CC Leiden, The Netherlands
[c] Prof. Dr. F. M. Bickelhaupt
Institute for Molecules and Materials (IMM), Radboud University,
Heyendaalseweg 135, 6525 AJ Nijmegen, The Netherlands
[‡] These authors contributed equally to this work
[+] These authors contributed equally to this work
Supporting information and ORCID(s) from the author(s) for this article are
available on the WWW under https://doi.org/10.1002/ejoc.202000590.

It is well known that the reaction conditions used for the ring-opening of non-symmetrical epoxides have a significant impact on the experimentally observed regioselectivity (Scheme 1).[3] Carrying out the reaction under basic conditions will lead to an attack of the nucleophile on the least hindered side of the epoxide (Scheme 1; β-attack). In contrast, under acidic conditions, the most substituted center of the epoxide will be attacked (Scheme 1; α-attack). The common explanation provided in textbooks is: (i) the regiochemical preference for the β-position in base-catalyzed reactions is ascribed to the steric interaction between the nucleophile and the epoxide;[1b,3a–3c,4] while (ii) the regioselectivity under acidic conditions is controlled by a more stabilized carbocation-like intermediate on the α-position.[3b–3d] Nonetheless, and despite recent studies on the mechanism of epoxide ring-opening reactions,[5] little quantitative data is available regarding the underlying physical factors behind the regioselectivity.

Scheme 1. Regioselectivity of epoxide opening reactions under basic and acidic conditions.

Here, we have performed an in-depth computational study to unravel the physical mechanism behind the regioselectivity of ring-opening reactions of the model non-symmetrical epoxide 2,2-dimethyloxirane under basic and acidic conditions. To simulate basic conditions, hydroxide (OH$^-$) will be used as nucleophile, while for acidic conditions, 2,2-dimethyloxirane will be protonated (2,2-dimethyloxiran-1-ium) and water (H$_2$O) will

serve as the nucleophile (Scheme 2).[6] The activation strain model (ASM)[7] in combination with Kohn–Sham molecular orbital (KS-MO)[8a] theory and the matching energy decomposition analysis (EDA)[8b,8c] were employed to provide quantitative insight into the factors controlling the regioselectivity of the nucleophilic substitution reactions. This methodological approach facilitates the analysis of the potential energy surface and, more importantly, the activation barrier, by decomposing the total energy of the system into chemically meaningful and easily interpretable terms, proving to be valuable for understanding the reactivity of, amongst others, nucleophilic substitution reactions.[9]
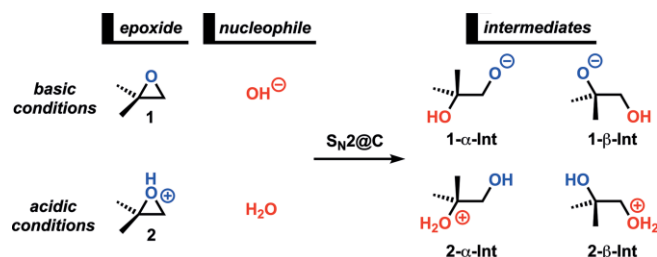
Scheme 2. Computationally analyzed ring-opening reactions of epoxide 1 under basic (1-α and 1-β) and 2 under acidic (2-α and 2-β) conditions.

Computational Method

Computational Details

All density functional theory (DFT) calculations were performed using the Amsterdam Density Functional (ADF2017.103) software package.[10] For all computations, the generalized gradient approximation (GGA) exchange-correlation functional OLYP was used, which consists of the optimized exchange (OPTX) functional proposed by Handy and co-workers,[11a,11b] and the Lee–Yang–Parr (LYP) correlation functional.[11c] In previous bench-

Thomas Hansen obtained his master degree (summa cum laude) in Chemistry from Leiden University in 2015. Directly after, he started his PhD research under the guidance of Dr. Jeroen Codée and Prof. Dr. Gijs van der Marel, in which he used a joint computational and experimental approach to study the glycosylation reaction mechanism. He is currently a postdoctoral fellow in the groups of Prof. Dr. F. Matthias Bickelhaupt and Dr. Trevor A. Hamlin at the Vrije Universiteit Amsterdam. His research interests lie at the intersection between organic and computational chemistry.

Pascal Vermeeren received his master's degree in Molecular Sciences from the Vrije Universiteit Amsterdam in 2017. At present, he is a PhD student under the supervision of Prof. Dr. F. Matthias Bickelhaupt and Dr. Trevor A. Hamlin in the Department of Theoretical Chemistry at the Vrije Universiteit Amsterdam. His scientific interests include elucidating the role of steric (Pauli) repulsion in chemical reactivity and molecular structures.

Anissa Haim is a BSc student (Chemistry) at the Vrije Universiteit Amsterdam and University of Amsterdam (expected graduation in 2020). In 2018 she joined the Theoretical Chemistry Department at Vrije Universiteit Amsterdam for a short research project together with Maarten van Dorp, under the supervision of Dr. Trevor A. Hamlin and Prof. Dr. F. Matthias Bickelhaupt. In 2020, she rejoined the Theoretical Chemistry Department to carry out her final BSc. research project, under the supervision of Dr. S. van der Lubbe and Prof. Dr. C. Fonseca Guerra.

Maarten J. H. van Dorp is currently a BSc. student chemistry at the Vrije Universiteit Amsterdam and the University of Amsterdam. In 2018, under the supervision of Dr. Trevor A. Hamlin and Prof. Dr. F. Matthias Bickelhaupt, he joined the Department of Theoretical Chemistry at the Vrije Universiteit Amsterdam for a short research project investigating epoxide ring-opening reactions together with Anissa Haim.

Jeroen Codée obtained his PhD from Leiden University developing new strategies for the synthesis of oligosaccharides and glycosaminoglycans in particular. After post-doctoral research at the ETH Zurich, developing microreactor chemistry and automated solid phase syntheses for peptides and carbohydrates, he returned to Leiden, where he runs the carbohydrate research group. His team develops synthetic methodology for the assembly of complex glycans and carbohydrate biosynthesis probes for glycobiology and glycoimmunology research. To enable these syntheses, computational chemistry is combined with experimental and spectroscopic techniques to unravel the complex glycosylation reaction mechanism.

F. Matthias Bickelhaupt holds Chairs in Theoretical Chemistry at Vrije Universiteit Amsterdam and Radboud University, Nijmegen, and is Head of the VU Department of Chemistry & Pharmaceutical Sciences. He is winner of the Dutch Research Council's VICI award, member of the Royal Holland Society for Sciences and Humanities, and Chemistry Europe Fellow. His research interests include developing the analysis and theory of chemical bonding and reactivity, with applications in organic, inorganic, and biological chemistry.

Trevor A. Hamlin obtained his B. S. in Biochemistry from Albright College (2010, cum laude) and his Ph.D. in Chemistry from The University of Connecticut (2015). In 2015, Trevor joined the Theoretical Chemistry Department at the Vrije Universiteit (VU) Amsterdam for his postdoctoral training. He secured an Assistant Professorship (with tenure) at the VU in 2018. The Hamlin research group leverages state-of-the-art computational methods to provide physical insight into the molecular reactivity of organic, inorganic, and biochemical reactions.

EurJOC
European Journal of Organic Chemistry

Full Paper
doi.org/10.1002/ejoc.202000590

Chemistry Europe
European Chemical
Societies Publishing

mark studies, we have shown that OLYP reproduces S_N2 barriers from highly correlated *ab initio* within only a few kcal mol^{-1}.[12] The basis set used, denoted TZ2P, is of triple-ζ quality for all atoms and has been improved by two sets of polarization functions.[13] The accuracies of the fit scheme (Zlm fit) and the integration grid (Becke grid) were, for all calculations, set to VERYGOOD.[14] Geometries were optimized without symmetry constraints. All calculated stationary points have been verified by performing a vibrational analysis,[15] to be energy minima (no imaginary frequencies) or transition states (only one imaginary frequency). The character of the normal mode associated with the imaginary frequency of the transition state has been analyzed to ensure that it is associated with the reaction of interest. Aqueous solvation was considered in the computations using the COSMO implicit solvation model. Solvent effects were explicitly used in the solving of the SCF equations and during the optimization of the geometry and the vibrational analysis.[16] The potential energy surfaces of the studied epoxide ring-opening reactions were obtained by performing intrinsic reaction coordinate (IRC) calculations,[17] which, in turn, were analyzed using the PyFrag program.[18] The optimized structures were illustrated using CYLview.[19]

Activation Strain and Energy Decomposition Analysis

The activation strain model (ASM) of chemical reactivity,[7] also known as the distortion/interaction model,[20] is a fragment-based approach in which the energy corresponding to a chemical reaction, *i.e.* the potential energy surface, can be described with respect to, and understood in terms of the characteristics of the reactants. It considers the rigidity of the reactants and to what extent they need to deform during the reaction plus their capability to interact with each other as the reaction proceeds. In this model, we decompose the total energy, $\Delta E(\zeta)$, into the respective total strain and interaction energy, $\Delta E_{strain}(\zeta)$ and $\Delta E_{int}(\zeta)$, and project these values onto the reaction coordinate ζ [Eq. (1)].

$$\Delta E(\zeta) = \Delta E_{strain}(\zeta) + \Delta E_{int}(\zeta) \tag{1}$$

In this equation, the total strain energy, $\Delta E_{strain}(\zeta)$, is the penalty that needs to be paid in order to deform the reactants from their equilibrium structure to the geometry they adopt during the reaction at point ζ of the reaction coordinate. The interaction energy, $\Delta E_{int}(\zeta)$, accounts for all the interactions that occur between these two deformed reactants along the reaction coordinate. The total strain energy can, in turn, be further decomposed into the strain energies corresponding to the deformation of the epoxide ring, $\Delta E_{strain,epoxide}(\zeta)$, and the nucleophile, $\Delta E_{strain,nucleophile}(\zeta)$ [Eq. (2)].

$$\Delta E_{strain}(\zeta) = \Delta E_{strain,epoxide}(\zeta) + \Delta E_{strain,nucleophile}(\zeta) \tag{2}$$

The interaction energy between the deformed reactants can be further analyzed in terms of quantitative Kohn–Sham molecular orbital theory (KS-MO) together with a canonical energy decomposition analysis (EDA).[8b] The EDA decomposes the $\Delta E_{int}(\zeta)$ into the following three physically meaningful energy terms [Eq. (3)]:

$$\Delta E_{int}(\zeta) = \Delta V_{elstat}(\zeta) + \Delta E_{Pauli}(\zeta) + \Delta E_{oi}(\zeta) \tag{3}$$

Herein, $\Delta V_{elstat}(\zeta)$ is the classical electrostatic interaction between the unperturbed charge distributions of the (deformed) reactants and is usually attractive. The Pauli repulsion, $\Delta E_{Pauli}(\zeta)$, comprises the destabilizing interaction between occupied closed-shell orbitals of both fragments due to the Pauli principle. The orbital interaction energy, $\Delta E_{oi}(\zeta)$, accounts for polarization and charge transfer between the fragments, such as HOMO–LUMO interactions. We have recently written a detailed, step-by-step, guide on how to perform and interpret the ASM and EDA which can be found in reference 7a.

In both the activation strain diagrams and accompanied energy decomposition plots in this study, the energy terms are projected onto the carbon–leaving group (C–LG) distance. This critical reaction coordinate undergoes a well-defined change during the reaction from the reactant complex via the transition state to the product and is shown to be a valid reaction coordinate for studying S_N2 reactions.[21]

Voronoi Deformation Density

The atomic charge distribution was analyzed by using the Voronoi Deformation Density (VDD) method.[22] The VDD method partitions the space into so-called Voronoi cells, which are non-overlapping regions of space that are closer to nucleus A than to any other nucleus. The charge distribution is determined by taking a fictitious promolecule as reference point, in which the electron density is simply the superposition of the atomic densities. The change in density in the Voronoi cell when going from this promolecule to the final molecular density of the interacting system is associated with the VDD atomic charge Q. The VDD atomic charge Q_A of atom A is calculated according to [Eq. (4)].

$$Q_A^{VDD} = -\int_{Voronoi\ cell\ of\ A} [\rho(r) - \rho_{promolecule}(r)]dr \tag{4}$$

So, instead of computing the amount of charge contained in an atomic volume, we compute the flow of charge from one atom to the other upon formation of the molecule. The physical interpretation is therefore straightforward. A positive atomic charge Q_A corresponds to the loss of electrons, whereas a negative atomic charge Q_A is associated with the gain of electrons in the Voronoi cell of atom A.

Thermochemistry

Bond enthalpies, *i.e.* bond dissociation energies (BDE), are calculated at 298.15 K and 1 atm (ΔH_{BDE}) from electronic bond energies (ΔE) and vibrational frequencies using standard thermochemistry relations for an ideal gas [Eq. (5)].[23]

$$\Delta H_{BDE} = \Delta E + \Delta E_{trans,298} + \Delta E_{rot,298} + \Delta E_{vib,0} + \Delta(\Delta E_{vib,0})_{298} \tag{5}$$

Here, $\Delta E_{trans,298}$, $\Delta E_{rot,298}$, and $\Delta E_{vib,0}$ are the differences between the epoxide and the ring-opened diradical, which results from breaking either the C^α–O or C^β–O bond, in translational, rotational, and zero-point vibrational energy, respectively. The

EurJOC
European Journal of Organic Chemistry

Full Paper
doi.org/10.1002/ejoc.202000590

Chemistry Europe
European Chemical Societies Publishing

last term, $\Delta(\Delta E_{vib,0})_{298}$, is the change in the vibrational energy difference when going from 0 K to 298.15 K.

Results and Discussion

The reaction profiles of the epoxide ring-opening reactions at the α- and β-position under basic (**1**) and acidic (**2**) conditions, as well as their transition state structures, are shown in Figure 1. In line with experimental findings, we establish that the nucleophilic attack at the β-position is favored in basic-catalyzed reaction, whereas the attack at the more substituted α-position is preferred under acidic conditions. Nucleophilic attack under basic conditions at the β-position not only proceeds with an activation barrier that is almost 6 kcal mol^{-1} lower than for attack at the α-position, but it also results in a more stable intermediate. For the ring-opening reactions under acidic conditions, the differences in activation barriers, as well as the stability of the intermediates, are 6 kcal mol^{-1} in favor of the attack at the α-position. The computed regioselective preferences under both basic and acidic conditions also hold in water (Figure 1a; in parentheses).
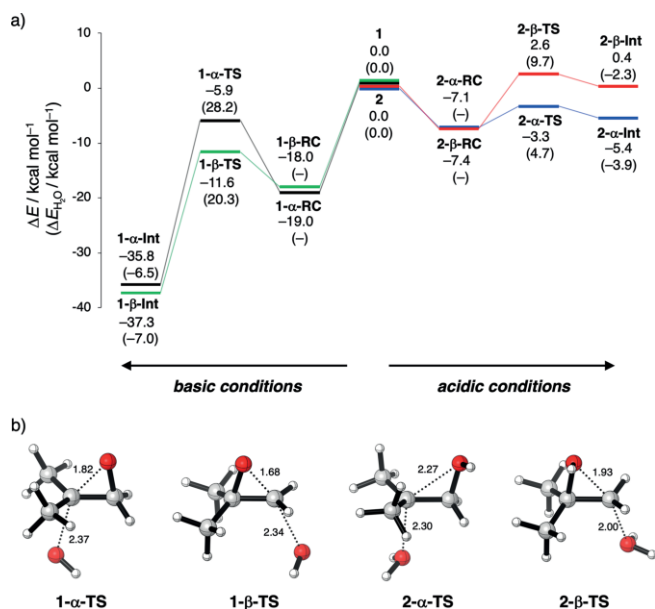

Figure 1. a) Reaction profiles for the base- and acid-catalyzed ring-opening reactions computed at OLYP/TZ2P and COSMO(H$_2$O)-OLYP/TZ2P; ΔE values computed in the gas-phase and in water (in parentheses; – is non-existing) in kcal mol^{-1}; and b) gas-phase transition state structures with key bond lengths (in Å) for the epoxide ring-opening of **1** and **2**.

In order to gain quantitative insight into the physical factors leading to the regioselectivity of the epoxide ring-opening reactions under acidic and basic conditions, we turned to the activation strain model (ASM) of reactivity.[7] First, we focus on the epoxide ring-opening reactions under basic conditions, as shown in Figure 2a. The preferred nucleophilic attack at the β-position of **1** originates solely from a more stabilizing interaction energy. Note that the strain energy shows a reversed trend, namely, **1-β** goes with a more destabilizing strain energy than **1-α**, which can be ascribed to their difference in computed bond strength (C$^{\alpha}$–O: ΔH_{BDE}= 57.5 kcal mol^{-1} and C$^{\beta}$–O: ΔH_{BDE}=

62.8 kcal mol^{-1}), but this is overruled by the regioselective preference established by the strong interaction energy.
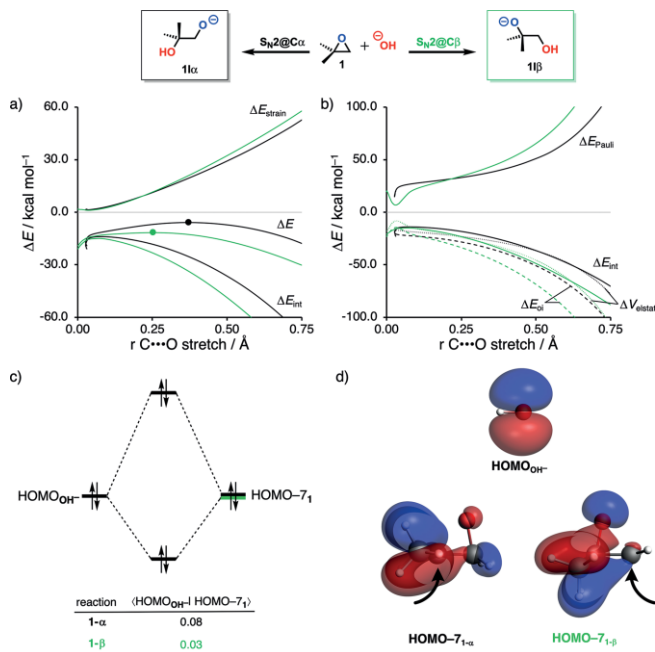

Figure 2. a) Activation strain analysis; and b) energy decomposition analysis of the base-catalyzed ring-opening reaction of **1**, where the energy values are projected on the C···O bond stretch; (c) molecular orbital diagram of the most important occupied–occupied orbital overlap of the base-catalyzed ring-opening reaction of **1**; and (d) key occupied orbitals (isovalue = 0.03 au$^{-3/2}$) computed at consistent geometries with a C···O bond stretch of 0.37 Å and an OH^{-}···C bond length of 2.19 Å. Computed at OLYP/TZ2P.

To understand why the attack at the β-position goes with a more stabilizing interaction energy compared to the attack at the α-position, we performed a canonical energy decomposition analysis (EDA).[8b] In analogy with the textbook explanation behind the regioselectivity of epoxides in base-catalyzed ring-opening reactions, we find that the steric (Pauli) repulsion is the driving force behind the preferred attack at the β-position. In Figure 2b, the steric (Pauli) repulsion is initially less destabilizing for **1-β**. Nevertheless, along the reaction coordinate the ΔE_{Pauli} curves intersect, resulting in more destabilizing ΔE_{Pauli} for **1-β**. One might be tempted to conclude that the regioselectivity is determined instead by the stabilizing orbital interactions combined with more stabilizing electrostatic interactions. However, we note that the EDA results are highly dependent on the OH^{-}···C$^{\alpha/\beta}$ distance (*vide infra*), which is almost 0.2 Å longer for **1-α** compared to **1-β** (2.38 Å for **1-α** and 2.19 Å for **1-β**) at a C···O bond stretch of 0.37 Å. The longer OH^{-}···C$^{\alpha}$ bond length is the result of greater steric bulk at C$^{\alpha}$ compared to C$^{\beta}$, which effectively causes all EDA terms to be smaller in absolute magnitude (*i.e.* a less destabilizing Pauli repulsion, in addition to less stabilizing orbital and electrostatic interactions).

To remedy this and account for the effect of the different nucleophile–substrate bond lengths on the EDA terms, we artificially constrained the OH^{-}···C$^{\alpha}$ bond length of **1-α** to the OH^{-}···C$^{\beta}$ bond length of **1-β** (2.19 Å), while keeping the C···O

EurJOC
European Journal of Organic Chemistry

Full Paper
doi.org/10.1002/ejoc.202000590

Chemistry Europe
European Chemical Societies Publishing

bond stretch consistent (0.37 Å). As expected, shortening of the OH⁻···C^α bond to 2.19 Å for **1-α** results in a significantly more destabilizing steric (Pauli) repulsion ($\Delta\Delta E_{Pauli}$ = 17.8 kcal mol⁻¹) together with a slightly less stabilizing orbital interactions ($\Delta\Delta E_{oi}$ = –0.8 kcal mol⁻¹) compared to **1-β** (See Table 1). The differences in ΔE_{Pauli} can be explained by performing a Kohn–Sham molecular orbital (KS-MO) analysis.[8a,24] We have quantified the key occupied–occupied orbital interaction between the π-HOMO of OH⁻ ($HOMO_{OH}^-$) and a filled σ-bonding orbital predominantly located on the methyl substituents of **1** ($HOMO–7_1$) that determine the trend in Pauli repulsion between the two reactants at consistent geometries with a C···O bond stretch of 0.37 Å and an OH⁻···C bond length of 2.19 Å. (Figure 2c and Figure 2d). Unsurprisingly, the attack at the α-position goes with a larger destabilizing orbital overlap with the methyl substituents than the attack at the β-position (0.08 and 0.07 for **1-α**; and 0.03 and 0.05 for **1-β**), because OH⁻ is in closer contact with the methyl substituents and, therefore, leads to more destabilizing steric (Pauli) repulsion. In order to relieve this highly destabilizing steric (Pauli) repulsion of **1-α**, the OH⁻···C^α bond will be elongated, even though this leads to a loss of stabilizing orbital and electrostatic interactions. This, in turn, gives rise to less stabilizing interaction energy and a higher activation barrier than **1-β**.

Table 1. Activation strain and energy decomposition analyses (in kcal mol⁻¹) for the epoxide ring-opening of **1** at the α- and β-position.[a]

	ΔE^*	ΔE_{strain}	ΔE_{int}	ΔV_{elstat}	ΔE_{Pauli}	ΔE_{oi}
1-α	–5.2	19.3	–24.5	–41.7	64.9	–47.7
1-β	–12.8	21.6	–34.4	–33.0	47.1	–48.5

[a] Analyses at consistent geometries with a C···O bond stretch of 0.37 Å and an OH⁻···C bond length of 2.19 Å. Computed at OLYP/TZ2P.

Furthermore, we found that the less favorable orbital interactions for **1-α** are due to both a higher-lying acceptor orbital, leading to a larger $HOMO_{OH}^-$–$LUMO_{1-C\alpha}$ orbital energy gap, and a worse $HOMO_{OH}^-$–$LUMO_{1-C\alpha}$ orbital overlap (see Figure S1a). The difference in orbital overlap was traced to the spatial extent of $LUMO_{1-C\alpha}$ and $LUMO_{1-C}^\beta$ (see Figure S1b). It can clearly be seen that the orbital lobe located at the β-position is significantly larger than the corresponding lobe on the α-position, due to two nodal planes between the lobe on the α-position and the two methyl groups, which, in turn, leads to a less favorable orbital overlap with the incoming nucleophile and less stabilizing orbital interactions. Thus, the pathway with the most favorable interactions, *i.e.*, less steric (Pauli) repulsion and slightly more orbital interactions, (β-attack) dominates under conditions of strong interactions (basic regime).

Next, we turned to the epoxide ring-opening reactions under acidic conditions, where the attack at the α-position is favored over the β-position. By applying the ASM, we found that the regioselectivity under acidic conditions is caused by differences in the strain energy (Figure 3a). The nucleophilic attack at the α-position goes with considerably less destabilizing strain energy compared to the attack at the β-position. The weak interaction energy is, in contrast with the prior discussed reaction under basic conditions, not able to overcome the regioselectivity set by the strain energy, because water is a weaker nucleophile than

OH⁻. To understand the origin of the strain energy, we have decomposed the total strain energy into the strain energies of the separate reactants, according to Equation (2) (Figure 3b). The less destabilizing strain energy of the attack at the α-position is exclusively caused by the predistortion of **2**. Under acidic conditions, the epoxide is protonated, leading to an asymmetric C–O bond elongation (C^α–O = 1.71 Å and C^β–O = 1.49 Å), because the C^α–O bond is weaker than the C^β–O bond (vide supra). This predistorts **2** more towards the product of the attack at the α-position and translates into less strain energy of this respective reaction mode (Figure 3c). This can be seen as the result of the earlier reported more stabilized carbocation-like intermediate on the α-position.[3b–3d] Upon protonation of the epoxide, the net positive charge accumulates at the more sterically encumbered (tertiary) α-carbon (Figure 3c; $VDD_{C\alpha}$: +0.110; $VDD_{C\beta}$: +0.014),[25] which results in a more stabilized carbocation-like species and, as a consequence, an elongation of the C^α–O bond. Altogether, the less destabilizing activation strain is significant enough to overcome the less stabilizing interaction energy for **2-α** compared to **2-β**, and therefore, the epoxide ring-opening reaction prefers to occur at the α-position. Thus, the least strained pathway (α-attack) dictates under conditions of weak interactions (acidic regime).

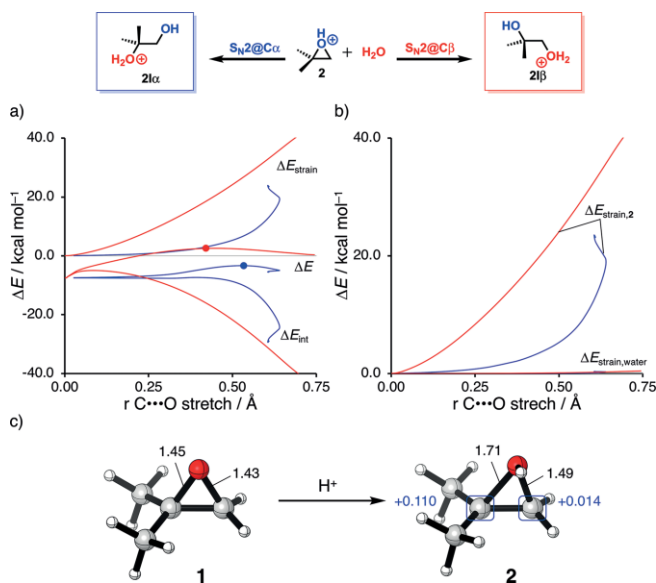

Figure 3. a) Activation strain analysis of the ring-opening reaction of **2**; b) strain decomposition where the energy values are projected on the C···O bond stretch; and c) ground-state geometries of epoxide **1** and **2** with the C–O bond lengths (black text, in Å) and the Voronoi deformation density (VDD, blue text) charges of the α- and β-position. Computed at the OLYP/TZ2P.

Importantly, our findings can also be generalized for the S_N1 pathway, which can be in competition with the S_N2 pathway,[5b,25,26] depending on the substitution pattern, under acidic conditions. The S_N1 pathway is a two-step mechanism where first the C–O bond is broken and a carbocation intermediate is formed (rate-determining step), followed by a nucleophilic attack at the carbocation. During the first step, the weaker C^α–O bond is more easily broken, resulting in less strain energy, than the stronger C^β–O bond, and a ring-opened inter-

EurJOC
European Journal of Organic Chemistry

Full Paper
doi.org/10.1002/ejoc.202000590

Chemistry
Europe
European Chemical
Societies Publishing

mediate is formed, which is the ultimate example of a predistorted epoxide. The following attack of the nucleophile at the carbocation C^α is then governed by orbital and electrostatic interactions. In other words, independent of the reaction pathway (S_N2 or S_N1), the nucleophile will attack at the α-position, in the gas phase under acidic conditions.

Conclusions

The regioselectivity of ring-opening reactions of non-symmetrical epoxides is highly dependent on the reaction conditions. We found, in line with previous studies, that the nucleophilic attack at the β-position of the epoxide ring is preferred under basic conditions, while the attack at the more sterically hindered α-position is favored under acidic conditions.

Our activation strain analysis revealed the underlying physical mechanisms behind the regioselectivity of the herein studied ring-opening. We found that under basic conditions, the regioselectivity is indeed caused by steric interactions. When the nucleophile attacks at the more sterically hindered α-position, the nucleophile undergoes significant steric (Pauli) repulsion with the methyl substituents of the epoxide. This reduces the stabilizing interaction energy and, therefore, raises the activation barrier than the β-attack. Thus, β-attack prevails in this interaction-controlled basic regime.

This changes under acidic conditions. Here, the nucleophile is water which interacts much weaker with epoxide than hydroxide. The control now shifts from the nucleophile–epoxide interaction to the epoxide activation strain which is more favorable, *i.e.* less destabilizing, as the weaker C^α–O bond dissociates upon α-attack. Protonation of the epoxide weakens both C–O bonds in the epoxide but the C^α–O bond always remains the weaker one. This is equivalent to the notion that the resulting carbocation intermediate is more substituted and thus more stabilized. The herein presented results solidly explain the physical factors behind the regioselectivity of ring-opening reactions of non-symmetrical epoxides.

Acknowledgments

[1] a) A. Padwa, S. Murphree, *ARKIVOC* **2006**, *3*, 6; b) J. G. Smith, *Synthesis* **1984**, *1984*, 629; c) P. Crotti, M. Pineschi, in *Aziridines and Epoxides in Organic Synthesis*, Wiley, Hoboken, **2006**, pp. 271–313.

[2] a) C. Schneider, *Synthesis* **2006**, *23*, 3919; b) I. Vilotijevic, T. F. Jamison, *Angew. Chem. Int. Ed.* **2009**, *48*, 5250; *Angew. Chem.* **2009**, *121*, 5352; c) A. Rolfe, T. B. Samarakoon, P. R. Hanson, *Org. Lett.* **2010**, *12*, 1216; d) B. M. Loertscher, Y. Zhang, S. L. Castle, *Beilstein J. Org. Chem.* **2013**, *9*, 1179.

[3] a) F. A. Carey, R. J. Sundberg, *Advanced Organic Chemistry Part A: Structure and Mechanisms*, Edn. 5, Springer, **2007**, pp. 511–515; b) F. A. Long, J. G. Pritchard, *J. Am. Chem. Soc.* **1956**, *78*, 2663; c) H. C. Chitwood, B. T. Freure,

[4] a) M. Muehlbacher, C. D. Poulter, *J. Org. Chem.* **1988**, *53*, 1026; b) T. Masamune, S. Sato, A. Abiko, M. Ono, A. Murai, *Bull. Chem. Soc. Jpn.* **1980**, *53*, 2895.

[5] a) R. C. D. Muniz Filho, S. A. A. de Sousa, F. da Silva Pereira, M. M. C. Ferreira, *J. Phys. Chem. A* **2010**, *114*, 5187; b) X. Li, Z. Yang, J. Xu, *Curr. Org. Synth.* **2013**, *10*, 169.

[6] L. P. Wolters, Y. Ren, F. M. Bickelhaupt, *ChemistryOpen* **2014**, *3*, 29.

[7] For a step-by-step protocol, see: a) P. Vermeeren, S. C. C. van der Lubbe, C. Fonseca Guerra, F. M. Bickelhaupt, T. A. Hamlin, *Nat. Protoc.* **2020**, *15*, 649; for reviews, see: b) F. M. Bickelhaupt, *J. Comput. Chem.* **1999**, *20*, 114; c) W.-J. van Zeist, F. M. Bickelhaupt, *Org. Biomol. Chem.* **2010**, *8*, 3118; d) I. Fernández, F. M. Bickelhaupt, *Chem. Soc. Rev.* **2014**, *43*, 4953; e) L. P. Wolters, F. M. Bickelhaupt, *WIRES Comput. Mol. Sci.* **2015**, *5*, 324; f) F. M. Bickelhaupt, K. N. Houk, *Angew. Chem. Int. Ed.* **2017**, *56*, 10070; *Angew. Chem.* **2017**, *129*, 10204.

[8] a) R. van Meer, O. V. Gritsenko, E. J. Baerends, *J. Chem. Theory Comput.* **2014**, *10*, 4432; b) F. M. Bickelhaupt, E. J. Baerends, in *Reviews in Computational Chemistry* (Eds.: K. B. Lipkowitz, D. B. Boyd), Wiley, Hoboken, **2000**, pp. 1–86; c) L. Zhao, M. von Hopffgarten, D. M. Andrada, G. Frenking, *WIRES Comput. Mol. Sci.* **2018**, *8*, e1345.

[9] For a review, see: a) T. A. Hamlin, M. Swart, F. M. Bickelhaupt, *ChemPhysChem* **2018**, *19*, 1315; b) T. A. Hamlin, B. van Beek, L. P. Wolters, F. M. Bickelhaupt, *Chem. Eur. J.* **2018**, *24*, 5927; c) T. Bettens, M. Alonso, F. De Proft, T. A. Hamlin, F. M. Bickelhaupt, *Chem. Eur. J.* **2020**, *26*, 3884.

[10] a) *ADF2017*, SCM, Theoretical Chemistry, Vrije Universiteit, Amsterdam (The Netherlands), **2017**; b) G. te Velde, F. M. Bickelhaupt, E. J. Baerends, C. Fonseca Guerra, S. J. A. van Gisbergen, J. G. Snijders, T. Ziegler, *J. Comput. Chem.* **2001**, *22*, 931; c) C. Fonseca Guerra, J. G. Snijders, G. te Velde, E. J. Baerends, *Theor. Chem. Acc.* **1998**, *99*, 391.

[11] a) J. B. Lucks, A. J. Cohen, N. C. Handy, *Phys. Chem. Chem. Phys.* **2002**, *4*, 4612; b) N. C. Handy, A. J. Cohen, *Mol. Phys.* **2001**, *99*, 403; c) C. T. Lee, W. T. Yang, R. G. Parr, *Phys. Rev. B* **1988**, *37*, 785.

[12] a) A. P. Bento, M. Solà, F. M. Bickelhaupt, *J. Chem. Theory Comput.* **2008**, *4*, 929; b) A. P. Bento, M. Solà, F. M. Bickelhaupt, *J. Comput. Chem.* **2005**, *26*, 1497.

[13] E. van Lenthe, E. J. Baerends, *J. Comput. Chem.* **2003**, *24*, 1142.

[14] a) M. Franchini, P. H. T. Philipsen, E. van Lenthe, L. Visscher, *J. Chem. Theory Comput.* **2014**, *10*, 1994; b) M. Franchini, P. H. T. Philipsen, L. Visscher, *J. Comput. Chem.* **2013**, *34*, 1819.

[15] a) A. Bérces, R. M. Dickson, L. Fan, H. Jacobsen, D. Swerhone, T. Ziegler, *Comput. Phys. Commun.* **1997**, *100*, 247; b) H. Jacobsen, A. Bérces, D. P. Swerhone, T. Ziegler, *Comput. Phys. Commun.* **1997**, *100*, 263; c) S. K. Wolff, *Int. J. Quantum Chem.* **2005**, *104*, 645.

[16] a) A. Klamt, G. Schüürmann, *J. Chem. Soc., Perkin Trans. 2* **1993**, 799; b) A. Klamt, *J. Phys. Chem.* **1995**, *99*, 2224; c) A. Klamt, V. Jonas, *J. Chem. Phys.* **1996**, *105*, 9972; d) C. C. Pye, T. Ziegler, *Theor. Chem. Acc.* **1999**, *101*, 396.

[17] a) K. Fukui, *Acc. Chem. Res.* **1981**, *14*, 363; b) L. Deng, T. Ziegler, L. Fan, *J. Chem. Phys.* **1993**, *99*, 3823; c) L. Deng, T. Ziegler, *Int. J. Quantum Chem.* **1994**, *52*, 731.

[18] X. Sun, T. M. Soini, J. Poater, T. A. Hamlin, F. M. Bickelhaupt, *J. Comput. Chem.* **2019**, *40*, 2227.

[19] C. Y. Legault, *CYLview*, Unversité de Sherbrooke, Sherbrooke, QC (Canada), **2009**.

[20] a) D. H. Ess, K. Houk, *J. Am. Chem. Soc.* **2007**, *129*, 10646; b) D. H. Ess, K. Houk, *J. Am. Chem. Soc.* **2008**, *130*, 10187.

[21] a) B. Galabov, G. Koleva, H. F. Schaefer III, W. D. Allen, *Chem. Eur. J.* **2018**, *24*, 11637; b) M. A. van Bochove, G. van Roos, C. Fonseca Guerra, T. A. Hamlin, F. M. Bickelhaupt, *Chem. Commun.* **2018**, *54*, 3448; c) B. van Beek, M. A. van Bochove, T. A. Hamlin, F. M. Bickelhaupt, *Electron Struct.* **2019**, *1*, 024001.

[22] C. Fonseca Guerra, J. W. Handgraaf, E. J. Baerends, F. M. Bickelhaupt, *J. Comput. Chem.* **2004**, *25*, 189.

[23] a) P. W. Atkins, J. de Pauli, *Physical Chemistry*, Edn. 9, Oxford University Press, Oxford, **2010**; F. Jensen, *Introduction to Computational Chemistry*, Edn. 2, Wiley, West Sussex, **2007**.

[24] T. A. Albright, J. K. Burdett, W. H. Wangbo, *Orbital Interactions in Chemistry*, Wiley, New York, **2013**.

[25] a) G. A. Olah, P. v. R. Schleyer, *Carbonium Ions*, Vol. 2, Wiley, New York, **1969**; b) M. B. Smith, *March's Advanced Organic Chemistry: Reactions, Mechanisms, and Structure,* 7th ed. Wiley, New York, **2013**; c) F. A. Carey, R. J. Sundberg, *Advanced Organic Chemistry, Part A*, Plenum Press, New York, **1984**.

[26] a) T. W. Bentley, P. v. R. Schleyer, *J. Am. Chem. Soc.* **1976**, *98*, 7658; b) F. K. Schadt, T. W. Bentley, P. v. R. Schleyer, *J. Am. Chem. Soc.* **1976**, *98*, 7667.